MODELING BLAST MOVEMENT FOR GRADE CONTROL

Isaaks E, Ph.D., MausIMM, Geostatistical Consultant, Isaaks & Co., Emerald Hills, CA 94062, USA. Email; ed@isaaks.com

Barr R, MAusIMM, MAIG, Senior Mine Geologist, Newmont Boddington Gold, PO Box 48, Boddington WA, 6390. Email; Robert.Barr@newmont.com

Handayani O, Lead Project Geologist, Newmont Boddington Gold, PO Box 48, Boddington WA, 6390. Email; Onie.Handayani@newmont.com

ABSTRACT

The mining industry has focused a great deal of attention recently on the impact of blast movement on grade control. Although the problem of blast movement and its contribution to dilution and ore loss is well known, solutions to the problem are less than satisfactory. Perhaps the most recent innovation is the application of blast movement monitoring (BMM) devices to quantify blast movement. These devices emit an electronic signal and are planted at surveyed locations within the pre-blast material. Following the blast, their new locations are found using an electronic scanner. The magnitude and direction of the blast movement is given by the vectors between the pre- and post-blast BMM locations. However, it's not clear how the BMM vector data can be best used to minimize dilution and ore loss. One common solution is to displace pre-blast dig line polygons by distances indicated by the BMM vectors. However, studies of BMM vectors show that blast movement not only displaces material laterally but also mixes material internally within the bench, (Thornton 2009a).

This paper presents a method for modeling the post-blast muck pile that accounts for displacement and internal dilution using simulated annealing. The pre-blast ore control block model is re-blocked to 1 x 1 x 1 m sub-blocks. Each sub-block is displaced by simulated BMM vectors conditional to post-blast surface topography and blast initiation sequence data in addition to BMM vector data. The displaced sub-blocks are aggregated into new ore control model blocks whose grades are calculated from the contained sub-blocks. New dig lines are then designed on the post-blast muck pile model using the new ore control block model grades. A case study based on actual data is provided.

INTRODUCTION

Open pit grade control generally entails the sampling and assaying of Reverse Circulation or blast hole cuttings followed by the estimation of ore control model (OCM) block grades. The estimated OCM block grades are then used in turn to design surface polygons or dig lines that outline and separate various ore types and waste material for the purposes of mining. However, the design of dig lines is followed by blasting where the primary goal of the blast is to achieve suitable fragmentation for subsequent mining, crushing and grinding of the ore material. Although fragmentation may be acceptable, unfortunately the blast also displaces and internally mixes the contents of the *in situ* material which creates dilution and poses a problem for the accurate estimation of mined grade. As mine to mill studies often highlight, the per tonne cost of blasting is significantly lower than crushing and grinding, which creates a cost pressure to

increase powder factors to increase fragmentation and thus further displace and mix the ore types.

During the blast the ore type materials within the pre-blast dig lines are displaced by various distances and directions to new locations, (Thornton, 2009a). The broken material also occupies a larger volume than it did before the blast due to the creation of void space between fragments. Thus, following the blast, the pre-blast dig lines contain a mixture of ore types and waste and no longer enable accurate selective mining.

An obvious solution is to design new dig lines over the broken material. However, current blast movement monitoring methods do not model the displaced OCM blocks. As a result, any set of post-blast dig lines must be designed without the aid of a subsurface model of grade and ore type. The common solution to this problem is to modify the pre-blast dig lines with reference to displacement data collected from blast movement monitoring (BMM) devices, (La Rosa and Thornton, 2011). The pre-blast dig lines are simply translated using the displacement vectors obtained from the BMM devices. The pre-blast grade and tonnage data within the dig lines are assumed to remain constant. But the BMM monitoring devices also reveal that material at mid bench is generally displaced greater distances than material at the top and bottom of the bench, (Thornton, 2009a). Thus, the top and bottom material of an OCM block may be mixed with mid bench material from neighboring OCM blocks. The net result is an internal mixing of materials which dilutes the original *in situ* ore types. Obviously, a simple translation of the pre-blast dig lines fails to account for such internal dilution and swell. The net result is excessive dilution and ore loss at the time of mining.

This paper presents a method for modeling blast movement that uses BMM data, post-blast surface topography, and blast initiation sequence data to map the displacement of individual pre-blast OCM sub-blocks to new post-blast locations. The displaced OCM sub-blocks are used to re-calculate a post-blast OCM with new OCM block grades and surface topography that accounts for blast induced lateral displacement, swell, surface topography, and the internal dilution of ore types. These new block grades enable the design of new dig lines that provide more accurate estimates of the tonnes and grade of each ore type available for mining. The method is illustrated by a running example using blast movement data provided by Newmont Boddington Gold.

The Newmont Boddington Gold mine is located in Western Australia (Figure 1) and is situated within the Saddleback Greenstone Belt which lies in the south-eastern corner of the Archaean Yilgarn Craton. The greenstone belt comprises a steeply-dipping and extensively faulted sequence of sedimentary felsic to mafic volcanic and pyroclastic rocks that have been metamorphosed to greenschist–amphibolite facies. The belt is about 50 km long and eight km wide, and is surrounded by granitic and gneissic rocks. Principal units are the Hotham Formation (meta sediments), the Wells Formation (felsic), which is the main host of the economic mineralization at Boddington, and the Marradong Formation (mafic).

The Boddington deposit is divided into two portions, Wandoo South and Wandoo North, which correspond to the former Boddington and Hedges oxide pits.

Wandoo South is centered on a composite aphyric diorite stock, the Central Diorite. In contact with the stock are a series of volcanic and volcaniclastic rocks, ranging from porphyritic to tuffaceous in character. Thin units of volcaniclastic rocks (fragmental) consisting of angular to well-rounded diorite and andesite clasts ranging from fine ash to agglomerate sizes are common within and around the diorite stock. A series of fine-grained microdiorite dykes, ranging from a few centimeters to several meters wide, cross-cut andesite, diorite, and fragmental lithologies. Wandoo North is dominated by diorites, with lesser fragmental volcanic rocks. The diorites and andesites are the preferred host lithologies for mineralization, with lesser mineralization recorded in the fragmental rock types and microdiorites. A series of post mineralization dolerite dykes cross cuts the entire Wandoo Resource area.

The andesites and diorites are extremely hard with typical uniaxial compression strengths between 100 and 250 MPa. Typical powder factors range from 1.2 to 1.4 kg/m^3. Blast movement distances measured by BMM devices average 13 m with standard deviations approaching 4 m. The minimum mining width is 15 m. Thus, it can be seen that blast movement and the associated mixing/dilution is a problem for grade control.

Figure 1: Newmont Boddington Gold mine site location

The outline of the paper is as follows. A description of the blast movement data provided by Newmont Boddington Gold is initially presented. The data includes:

- the ore control block model (OCM);
- blast movement monitoring (BMM) data;
- blast initiation sequence data; and
- post-blast surface topography.

Following this, the method used to simulate blast movement conditional to the blast movement data described above is presented. Finally, an application to grade control and the monetary gain attributable to modeling blast movement is presented.

NEWMONT BODDINGTON GOLD BLAST MOVEMENT DATA

The Ore Control Block Model (OCM)

The OCM for this study consists of 857 blocks each measuring 5 x 5 x 12 m. Each block is populated with a copper and gold grade as well as a $/ton value. The grades and revenue values have been transformed to a single gold (g/t) value to preserve confidentiality. (Cutoff grades and recovery rates used in this example are not equivalent to the actual values used by Newmont Boddington Gold.) Rock density is 2.75. Figure 2 shows a plan view of the OCM. Table 1 provides OCM grade and ore type statistics before dig line design.

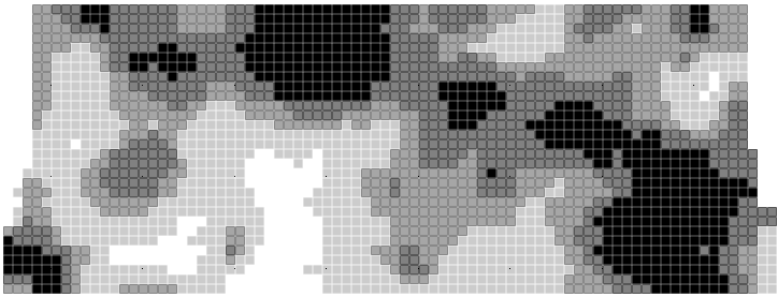

Figure 2: A plan view of the pre-blast ore control block model. Black is very high grade ore (VHG), dark grey is high grade (HG), medium grey is medium grade(MG), and light grey is low grade (LG) ore type.

Table 1: Statistics of the Ore Control Block Model

Ore Type	Cutoff (g/t)	Average Grade (g/t)	Tonnes
Waste	0.0	0.200	71,280
Low Grade (LG)	0.40	0.483	185,625
Medium Grade (MG)	0.56	0.607	161,865
High Grade (HG)	0.67	0.746	160,083
Very High Grade (VHG)	0.85	1.008	133,353

The 857 OCM blocks were subsequently divided into 257,100 unit blocks or voxels, each measuring 1 x 1 x 1 m. Each voxel was assigned the transformed gold grade (g/t) of its parent block.

The Blast Movement Monitoring (BMM) Database

The Newmont Boddington Gold BMM data base contains 1,515 BMM observations. Approximately 35 variables are recorded for each observation. These included items such as collar coordinates, depth from top, movement vector, powder factor, initiation pattern, rock type, pit zone and so on.

The horizontal displacements of BMM vectors were classified into 5 statistically independent groups based on corresponding geologic and blast data by a statistical algorithm known as *classification and regression trees*. Each of the 5 groups has a characteristic distribution of horizontal displacements as shown in Figure 3. An ANOVA test shows that the means of the 5 groups are statistically independent from one another with the exception of groups 2 and 3. Note that the shapes of the histograms resemble a normal distribution which is convenient for modeling purposes. The key variables used to classify the horizontal displacements into 5 groups are rock type, pit location, and blast initiation pattern. Interestingly, powder factor did not rank amongst the top classification predictors.

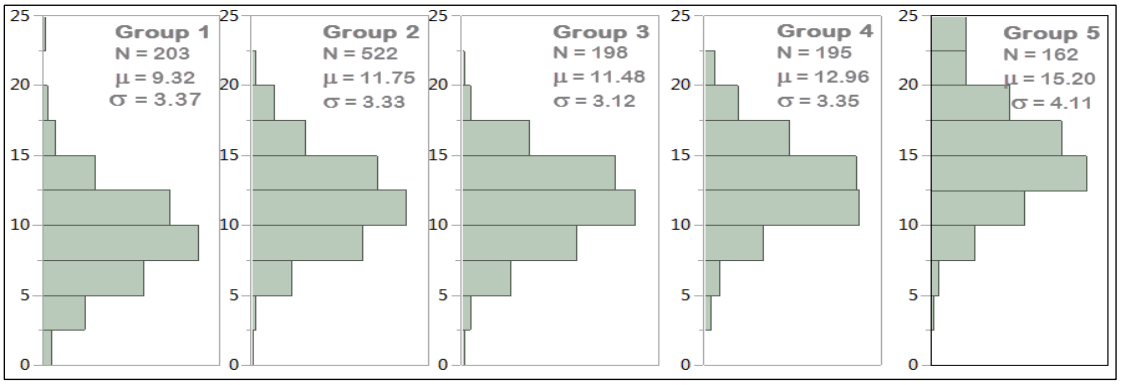

Figure 3: This figure shows the histogram, mean, and standard deviations of the BMM horizontal displacements for each of the 5 statistical groups.

Figure 4 shows a scatterplot of *horizontal displacement* versus *depth from the top* (of the bench) data for group 5. The curve in the figure is a polynomial regression line or predicted horizontal displacement as a function of depth from the top. For example, the horizontal displacement is approximately 15 m at 6 m from the top (mid-bench) while it is less than 10 m at the top and bottom of the bench. The marginal histogram on the Y-axis shows the distribution of horizontal displacement for group 5. Polynomial regression curves for the other 4 groups showed greater displacements at mid bench than at the top and bench bottoms, however the differences are not as great as that in group 5.

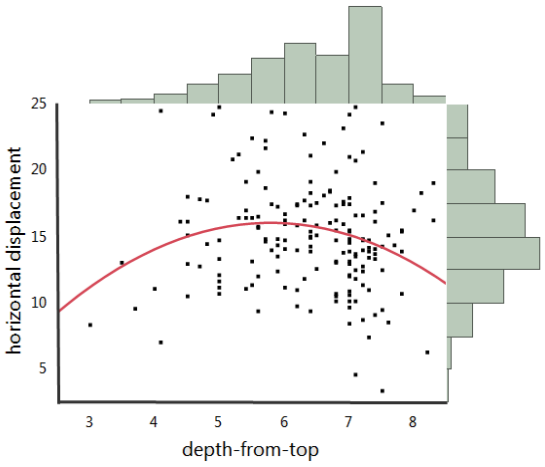

Figure 4: This figure shows the relationship between horizontal movement and depth from the top for Group5. Note the horizontal displacement is approximately 15 m at mid bench (6 m from the top) while it is less than 10 m at the top and bottom of the bench.

Note the large scatter of horizontal displacements in Figure 4. For example the figure shows displacements range from 4 to 25 m. Figure 3 shows the standard deviations range from 3.33 to 4.11. The high variance of horizontal displacements suggests that a simple translation of the pre-existing dig lines is likely an inadequate method for designing post-blast dig lines.

Blast Initiation Sequence Data

The blast initiation sequence data provided by Newmont Boddington Gold consists of a file containing the collar coordinates and detonation times for 791 blast holes. Figure 5 shows a map of the blast holes with contours of equal detonation times. The figure shows the blast was wired in a typical "V" pattern. The two large arrows in the figure show the theoretical directions of blast movement.

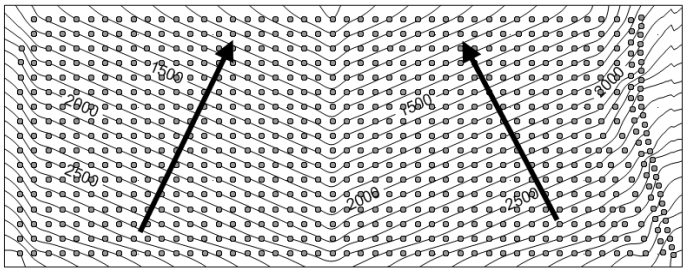

Figure 5: This figure shows a map of the blast holes covering the *in situ* ore control model for this study. Detonation time contours have been added to show the theoretical direction of blast movement.

Post-blast Surface Topography

The post-blast surface topography was measured by Newmont Bodding Gold using a Maptek I-Site 8810 laser scanner. The surface topography data consists of 32,736 elevation grid points on a nominal 1 x 1 m grid. Figure 6 shows a map of the post-blast surface topography. The map also shows the location of the blast holes comprising the blast. Note the post-blast surface topography extends beyond the blast holes in the upper part of the figure as a result of the blast movement.

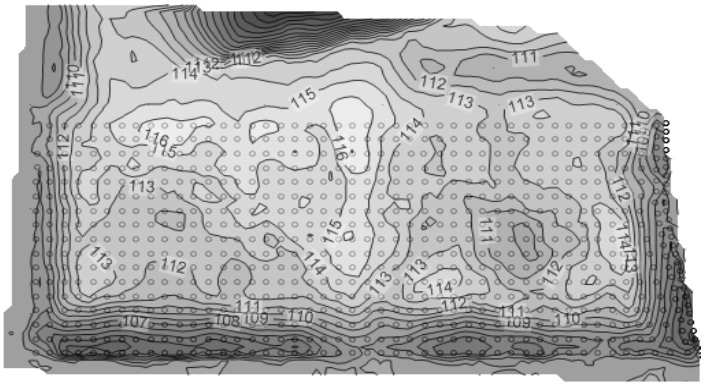

Figure 6: This figure shows a contour map of the post-blast surface topography. The small circles indicate the location of blast holes. The contours run from an elevation of 98 m ASL in the power trough to 117 m ASL at the peak of the topography for a *trough to peak* elevation difference of 19 m.

MODELING BLAST MOVEMENT – THE METHOD

The method used to model blast movement can be described in general as follows:

1. sub-block the pre-blast OCM into unit cubes (voxels);
2. define a post-blast envelope bound by the post-blast surface topography and bench floor elevations ;
3. define a regular grid within the post-blast envelope where the number of grid points is equal to the number of voxels defined in (1);
4. assign movement directions to each pre-blast voxel;
5. assign a distribution of potential horizontal displacements to each pre-blast voxel; and
6. simulate a horizontal displacement for each voxel conditional to the distribution of displacements and movement directions previously assigned to the voxel.

The following sections describe each step in greater detail.

Sub-Block the Pre-blast OCM

As indicated above, the *in situ* or pre-blast OCM shown in Figure 2 consists of 857 blocks, each measuring 5 x 5 x 12 m. Thus, the total volume of the pre-blast OCM is 5 x 5 x 12 x 857 or 257,100 cubic meters. Each cubic meter can be considered to be a voxel or 3 dimensional pixel. With some simple calculations, each voxel can be assigned (x,y,z) centroid coordinates and the grade (g/t) of its parent OCM block. To summarize, these calculations result in a pre-blast OCM consisting of 257,100 voxels where each voxel has a volume of 1 cubic meter.

Define the Post-blast Envelope

The post-blast envelope is simply defined by the volume bound by the floor and post-blast surface topographies. For example, Figure 7 shows a cross section through the post-blast envelope. Given the elevations of the post-blast floor and upper surfaces, a simple calculation yields the volume of the post-blast envelope (354,798 cubic meter). Thus, the swell factor is given by the ratio of the volume of the post-blast envelope to the volume of the pre-blast OCM calculated to be 1.38 in this example.

By applying the swell factor to each of the 257,100 pre-blast voxels, the dimensions of a post-blast voxel can be calculated as the cubed root of 1.38 which is approximately 1.113 m. Thus, a regular 3 dimensional grid with grid nodes at 1.113 m intervals was calculated with overall dimensions slightly larger than those of the post-blast envelope. This oversize grid is subsequently clipped by the post-blast envelope surfaces leaving a total of 257,100 grid points within the post-blast envelope. Thus, each of the 257,100 pre-blast voxels can theoretically be displaced or moved to a unique location within the post-blast envelope without creating or losing a single ounce or tonne.

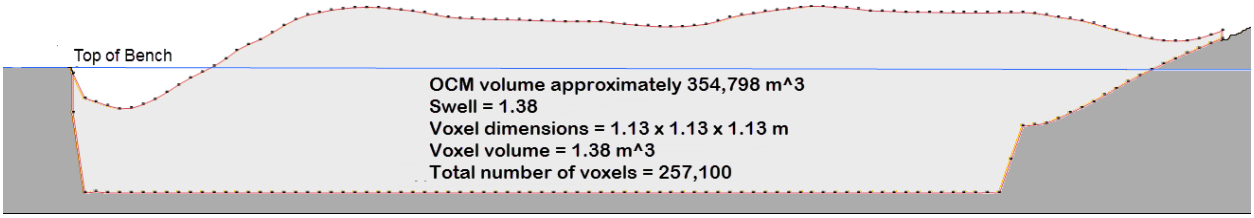

Figure 7: This figure shows a cross section through the post-blast muck pile. The light grey area denotes the post-blast envelope while the darker area shows material that is not part of the current post-blast envelope. The direction of blast movement is to the right.

Assign Blast Movement Directions to Pre-Blast Voxels

Blast movement directions are calculated perpendicular to the detonation time contours (Figure 5) and assigned to each of the 257,100 pre-blast voxels. Note that for the actual simulation of displacement, a small random angle is added to the movement direction initially assigned to each pre-blast voxel. Blast movement directions are also calculated and assigned to each of the 257,100 post-blast envelope grid nodes. The movement directions assigned to the post-blast envelope grid nodes are used to calculate the impact of collisions between pre-blast voxels traveling on collision paths due to the "V" blast pattern. This is done by monitoring the simulated movement of each pre-blast voxel to its new site or grid node within the post-blast envelope. The simulated movement direction of the pre-blast voxel is compared to the movement direction assigned to the envelope grid node. If the two directions indicate collision paths, the simulated displacement distance is modified according to the collision angle.

Assign Distributions of BMM Horizontal Displacements to Pre-Blast Voxels

Based on the data shown in Figures 3 and 4, a normal distribution of horizontal displacements is associated with each of the 257,100 pre-blast voxels. The mean and standard deviations vary with *depth from the top* with the largest mean and standard deviations at 6 m from the top of the bench or mid bench. Table 2 shows the mean and standard deviations at the top, mid, and bottom of the bench. The horizontal movement distance for each of the 257,100 voxels is simulated by a random draw from the distribution of displacements associated with each voxel. Thus, mid-bench voxels tend to be displaced greater distances than voxels at the top or bottom of the bench. The result is a vertical mixing of the unit voxels in the post-blast envelope and a corresponding dilution of ore types.

Table 2: Means and Standard Deviations
of Simulated Horizontal Displacement Distributions

Depth From Top	Mean(m)	Std. Dev.
1	8	3.0
6	12.6	4.0
12	6	3.0

Simulate Blast Movement

The simulation of blast movement is accomplished by displacing each of the 257,100 pre-blast voxels to a unique grid node in the post-blast envelope where the displacement is constrained by:

- the post-blast surface topography;
- the distribution of displacement distances associated with each voxel;
- the direction of displacement assigned to each voxel; and
- collisions with other voxels.

The final post-blast OCM is calculated by aggregating the unit post-blast voxels into a specified OCM block size. The post-blast OCM preserves the average grade and total tonnage of the pre-blast OCM and honors the post-blast surface topography. Theoretically, no ounces or tonnes are lost or added. In practice the differences seen between pre and post blast tonnes and ounces is less than 0.5%.

APPLICATION TO GRADE CONTROL

The grade control case study described here employs the grade control procedures utilized at Newmont Boddington Gold but not in all respects. For example, the recovery rates, minimum mining width and dig lines have been altered to preserve confidentiality.

The dig lines shown in this case study are calculated using Digger which is a computer program for the design of optimum dig lines given a minimum mining width constraint, (Isaaks, 2014). Using Digger for dig line design ensures design consistency between the pre-blast and post-blast dig lines and minimizes differences between the pre-blast and post blast recoveries that could be attributed to subjective dig line design.

Key grade control parameters are:

1. Gold Price = USD 38.58/gram.
2. Low grade recovery = 65%
3. Med Grade Recovery = 73%
4. High Grade Recovery = 81%
5. Very High Grade Recovery = 90%
6. Minimum mining width = 15 m
7. Broken material density = 2.00 g/cc

The cutoff grades defining the ore type classes and waste are given in Table 1.

Pre-Blast Dig Lines and Predicted Recoveries

Figure 8 provides a map of the pre-blast dig lines while Table 3 provides the statistics of the dig line ore types constrained by a 15 m minimum mining width. The impact of the pre-blast dig lines on ore loss and dilution can be seen by comparing Table 1 to Table 3.

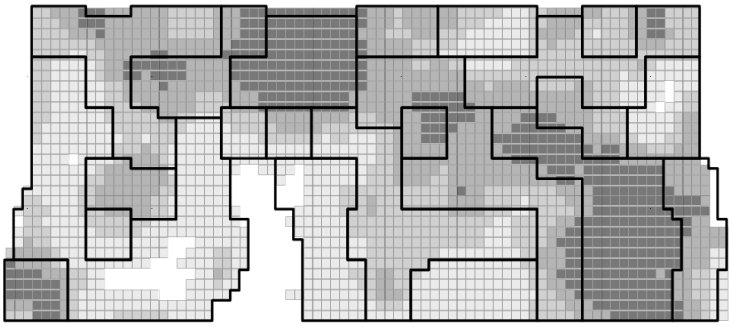

Figure 8: The solid black lines are the pre-blast dig lines designed on the pre-blast OCM (Figure 2) which is shown in the background. The minimum mining width is 15 m or 5 blocks (The OCM has been re-blocked to 3 x 3 m blocks to accommodate Digger).

Table 3: Pre-blast Dig Line Statistics

Ore Type	Tonnes	g/t
Waste	65,934	0.193
Low Grade	207,306	0.504
Med Grade	168,696	0.643
High Grade	167,805	0.760
Very High Grade	102,465	1.00
Total	712,206	0.640
Net Revenue (excl. waste)	$5,126,176	

Given that a common solution for the design of post-blast dig lines is a simple translation of the pre-blast dig lines and given that the tonnes and grade within the pre-blast dig lines are assumed

to be constant, the statistics in Table 3 provide the tonnes, grade, and net revenue that would be expected following the blast. For example, the mill could expect 102,465 tonnes of very high grade material at an average grade of 1.00 gram/tonne based on the pre-blast model data.

The Post-blast Model and Predicted Recoveries

The post-blast OCM blocks consist of 5 post-blast voxels in the X direction and 5 in the Y direction and a variable number of voxels in the Z direction due to the variable post-blast surface topography. Thus, the horizontal dimensions of the post-blast OCM blocks are approximately 5.65 x 5.65 m.

Because the post-blast OCM is an actual block model with block grades (where tonnes and metal content are preserved), it is possible to re-design new dig lines. This was done by applying Digger to the post-blast OCM block grades.

Figure 9 shows a map of the newly designed post-blast dig lines. Note that these dig lines take account of the variable block height. Obviously, a block that is 16 m high is twice as valuable as a block 8 m high given identical grades. The minimum mining width is 15 m. The post-blast OCM block grades are shown in the background. The correspondence between ore type and grey scale is identical to that described in Figure 2. The statistics of the Digger dig lines are given in Table 4.

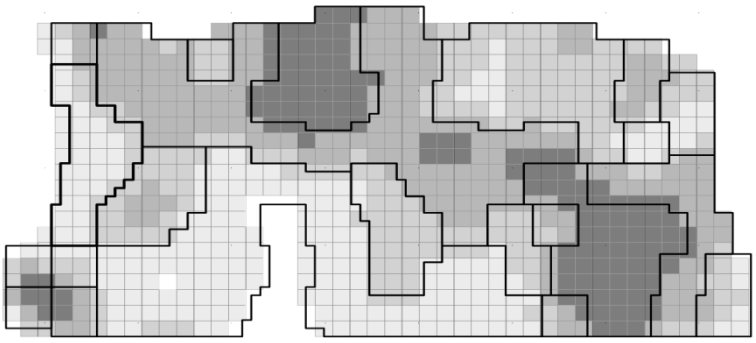

Figure 9: This figure shows a map of newly designed dig lines which overlie the post-blast OCM. These dig lines were designed by Digger. Note that the design of dig lines takes into account the variable OCM block height or block tonnages.

Table 4: Post-blast Dig Line Statistics

Ore Type	Tonnes	g/t
Waste	61,510	0.251
Low Grade	201,946	0.495
Med Grade	156,996	0.617
High Grade	200,340	0.766
Very High Grade	91,395	0.981
Total	712,187	0.639
Net Revenue (excl. waste)	$4,870,633	

A comparison of Table 4 with Table 3 is interesting because Table 4 shows the tonnes and grade of the post-blast OCM ore types available for mining whereas the mill is expecting the tonnes and grade shown in Table 3. For example, although the mill was expecting 102,465 tonnes of very high grade material at an average grade of 1.00 g/t (Table 3), only 91,395 tonnes of very high grade ore averaging 0.981 g/t are actually available for mining from the post-blast OCM (Table 4). Obviously, blast movement and internal mixing have diluted the very high grade ore type so that it is not possible to achieve the pre-blast grade predictions. Accordingly $5.13 million is expected from the entire blast, but only $4.87 million is realized. In other words, the pre-blast dig lines over predict net revenue by 5.2%. This suggests that the internal dilution of ore types due to blast movement is likely the source of many mine to mill reconciliation problems.

DISCUSSION AND RELATED WORK

A review of the literature on modeling blast movement for grade control reveals that most blast movement models are designed to simulate the complexity of a blast from the fundamentals of physics. (Schamaun, 1983; Yang and Kavetsky, 1990; Furtney**,** Cundall, and Chitombo, 2009; Preece, Burchell, and Scovira,1993; La Rosa and Thornton, 2011; Tordoir *et al,*2009). The blast movement modeling method presented in this paper is a simple mechanical method governed by actual physical data. The software developed to simulate blast movement executes in a few minutes. No attempt is made to understand or simulate the complexity of blasting from fundamental physics. However, if our method enables a more accurate selection of ore types at the time of mining, then we have achieved our goal.

CONCLUSIONS

The blast movement modeling method described here entails generation of a post-blast OCM that:

- contains block grades;
- preserves the tonnes and metal content seen in the pre-blast OCM;
- reproduces the post-blast surface topography;

- accounts for swell; and
- reproduces the characteristic displacement distributions and directions as seen in the BMM monitoring data.

Based on the post-blast OCM block grades, new dig lines can be designed that account for the internal mixing and dilution of ore types resulting from blast movement. The case study suggests that the internal dilution of ore types due to blast movement may reduce net revenue by as much as 5.2% and may be the source of many mine to mill reconciliation problems.

FUTURE WORK

The modeling method described here is very flexible. For example, since a characteristic distribution of displacement distances is uniquely associated with each pre-blast voxel, future work will not only customize the distribution of displacement distances as a function of depth from the top, but also as a function of location such as the front, body, and back of the blast. Distributions of displacement distances can also be customized voxel by voxel for specific blast patterns. More work will also be done to further quantify the degree of randomness associated with the theoretical movement directions suggested by blast initiation sequences.

In spite of the fact that the current method yields a post-blast model that reproduces displacement distances, displacement directions, post-blast surface topography, swell, and the *in situ* pre-blast OCM tonnage and metal content, model validation is thought to be necessary. Obviously, model validation will require confirmation of the post-blast dig line tonnages and grades. We are currently investigating several methods to accomplish this including planting numerous electronic markers in the bench prior to blasting. As the post-blast material is loaded by shovel, the electronic markers will also be retrieved by the shovel. A scanner mounted on the shovel bucket will detect the electronic marker and read the data encoded within the marker (grade, ore type, initial coordinates etc.). These data will be subsequently relayed to dispatch and/or a central data base. The post-blast location of the electronic marker will be provided by a shovel mounted GPS unit. A simple comparison between the electronic marker data and the post-blast dig line statistics will allow validation of the modeling method.

REFERENCES

Furtney, J, Cundall, P and Chitombo, G, 2009. Developments in numerical modeling of blast induced rock fragmentation: Updates from the HSBM project, in *Proceedings Ninth International Symposium on Rock Fragmentation by Blasting – Fragblast 9* (ed: J A Sanchidrian), (Taylor and Francis Group: London), pp 335-342.

Isaaks, E, Treloar, I, and Elenbaas, T, 2014. Optimum dig line design for grade control, in *Proceedings Ninth International Mining Geology Conference 2014*, (The Australasian Institute of Mining and Metallurgy: Adelaide).

La Rosa, D, and Thornton, D, 2011. Blast Movement Modelling and Measurement, in *proceedings of 35th APCOM Symposium*, Wollongong NSW, pp 297 – 309.

Preece, D S, Burchell, S L and Scovira, D S, 1993. Coupled explosive gas flow and rock motion modelling with comparison to bench blast field data, in *Proceedings Fourth International Symposium on Rock Fragmentation by Blasting – Fragblast 4* (ed: H P Rosmanith), (Balkema: Rotterdam), pp 239-245.

Schamaun, J.T., 1983. An Engineering Model for Predicting Rubble Motion During Blasting. in *Proceedings of 9th ConI. on Explosives & Blasting Techniques,* Soc. of Explosive Engineers, Dallas, TX, February.

Thornton, D M, 2009a. The implications of blast-induced movement to grade control, in *Proceedings Seventh International Mining Geology* Conference 2009, (Australasian Institute of Mining and Metallurgy: Melbourne), pp 147-154.

Thornton, D, Sprott, D and Brunton, I, 2005. Measuring blast movement to reduce ore loss and dilution, in *Proceedings 31st Annual Conference on Explosives and Blasting Technique* (International Society of Explosives Engineers: Cleveland).

Tordoir, A, Weatherley, D, Onederra, I and Bye, A, 2009. A new 3D simulation framework to model blast induced rock mass displacement using physics engines, in *Proceedings Ninth International Symposium On Rock Fragmentation By Blasting – Fragblast 9* (ed: J A Sanchidrian), (Taylor and Francis Group: London), pp 381-388.

Yang, R L and Kavetsky, A P, 1990. A three dimensional model of muck pile formation and grade boundary movement in open pit blasting, *International Journal of Mining and Geological Engineering 8*, (Springer: New York), pp 13-34.